Available online at www.sciencedirect.com

SciVerse ScienceDirect

Ceramics International 39 (2013) 6013–6017

CERAMICS INTERNATIONAL

www.elsevier.com/locate/ceramint

Short communication

High quantum efficiency red-emission tungstate based phosphor $Sr(La_{1-x}Eu_x)_2Mg_2W_2O_{12}$ for WLEDs application

Sheng Long[a,b], Jingshan Hou[a,c], Ganghua Zhang[a], Fuqiang Huang[a,*], Yi Zeng[b,**]

[a]CAS Key Laboratory of Materials for Energy Conversion, Shanghai Institute of Ceramics, Chinese Academy of Sciences, Shanghai 200050, PR China
[b]State Key Laboratory of High Performance Ceramics and Superfine Microstructure, Shanghai Institute of Ceramics, Chinese Academy of Sciences, Shanghai 200050, PR China
[c]College of Materials Science and Engineering, Donghua University, Shanghai 200051, PR China

Received 5 December 2012; received in revised form 6 January 2013; accepted 7 January 2013
Available online 16 January 2013

Abstract

A series of red-emitting Eu^{3+}-doped phosphors $SrLa_2Mg_2W_2O_{12}$ were successfully prepared by the solid state reaction and their luminescence properties were investigated in detail. Under 464 nm light excitation, the emission intensity at 613 nm increased with the Eu^{3+} ion concentration rising, and the quenching effect did not appear until the Eu^{3+} ion concentration reached 25%, and the critical distance was calculated to be 7.74 Å. The emission intensity of $Sr(La_{0.75}Eu_{0.25})_2Mg_2W_2O_{12}$ is approximately three times higher than that of the commercial red phosphor Y_2O_3:Eu^{3+} under the blue light, meanwhile, the quantum efficiency of $Sr(La_{0.75}Eu_{0.25})_2Mg_2W_2O_{12}$ is about two times higher than that of Y_2O_3:Eu^{3+}. The Commission Internationale de l′Eclairage chromaticity coordinate of $Sr(La_{0.75}Eu_{0.25})_2Mg_2W_2O_{12}$ is ($x=0.660$, $y=0.340$), which is closed to the standard of NTSC ($x=0.670$, $y=0.330$). The results indicate that $Sr(La_{1-x}Eu_x)_2Mg_2W_2O_{12}$ could be a potential red phosphor in fabrication of blue chips WLEDs.

Keywords: $Sr(La_{1-x}Eu_x)_2Mg_2W_2O_{12}$; Phosphor; Luminescence; Quantum efficiency

1. Introduction

White light emitting diodes (WLEDs) are an important light source with high efficiency, low power consumption, widespread applicability, extremely high durability and a long working life [1–4]. With an increasing concern for energy crisis and environment pollution, WLEDs have attracted substantial attention of researchers and significant progress has been made in relevant studies [4–7]. In consideration of the cost and complexity of the system, phosphor-converted WLEDs, which combine blue chips with yellow phosphors like YAG:Ce, are the most widely used commercialized solution [8]. However, this kind of WLEDs suffer from poor Commission Internationale de l′Eclairage (CIE) chromaticity coordinates and high color temperature because of the shortage of red light content [1,9]. Consequently, the low color render index value (R_a) limits WLEDs' applications when precise white light is required such as indoor illumination and screen display [10]. To warm the white light and improve the color render index, it is a promising strategy to combine red/green phosphors with blue chips, avoiding degradation of packaging materials aroused by UV light in UV-based LED [11–13]. At present, commercial red phosphors are mainly sulfides and nitrides. However, sulfides have a poor stability [14,15], whereas nitrides are usually very difficult to synthesize [13,16]. Thus, the development of stable oxide-based red phosphors is an urgent and important issue.

Tungstate complexes are self-activating phosphors with high stability and refractive index, which endow them to maintain efficient energy transfer from the host matrix to the localized states of the doping ions [17,18]. Previously, $SrLa_2Mg_2W_2O_{12}$ was reported to have an orthorhombic perovskite structure with a base-centered lattice and the lattice parameters of

*Corresponding author. Tel./fax: +86 21 5241 6360.
**Corresponding author.
Tel.: +86 21 5241 3108; fax: +86 21 5241 3107.
E-mail addresses: huangfq@mail.sic.ac.cn (F. Huang), zengyi@mail.sic.ac.cn (Y. Zeng).

0272-8842/$ - see front matter © 2013 Elsevier Ltd and Techna Group S.r.l. All rights reserved.
http://dx.doi.org/10.1016/j.ceramint.2013.01.013

$a=7.841$ Å, $b=7.858$ Å, and $c=7.893$ Å [19]. However, there are few reports about its applications and its rare earth ions doped derivatives as phosphors. Therefore, in the present study, we synthesized $Sr(La_{1-x}Eu_x)_2Mg_2W_2O_{12}$ via the high temperature solid state reaction, and their luminescence properties were investigated in detail. The results show that $Sr(La_{1-x}Eu_x)_2Mg_2W_2O_{12}$ could be a promising red phosphor applied in WLEDs.

2. Materials and methods

2.1. Sample preparation

Powder samples of $Sr(La_{1-x}Eu_x)_2Mg_2W_2O_{12}$ were prepared by the high temperature solid state reaction. Raw materials included $SrCO_3$ (A.R.), WO_3 (A.R.), $(MgCO_3)_4\cdot Mg(OH)_2\cdot 5H_2O$ (A.R.), and La_2O_3 (99.99%) were purchased from Sinopharm Chemical Reagent Co., Ltd. and Eu_2O_3 (99.99%) was purchased from Yixing Xinwei Group Co., Ltd. The stoichiometric amounts of the untreated reagents were weighed, mixed, and ground in an agate mortar with the help of acetone. Then, the mixture was transferred into the corundum crucible and calcined at 1450 °C for 24 h for complete reaction. Finally, the samples were cooled to room temperature by furnace cooling and grounded to powder for characterizations.

2.2. Characterization

To evaluate the purity and crystallinity of the samples, X-ray diffraction (XRD) was carried out using a Bruker D8 Focus Diffractometer with Cu $K\alpha$ radiation at a scanning speed of 6°/min with the range of 10–80°. Samples' photoluminescence excitation (PLE) and photoluminescence emission (PL) spectra were measured by Horiba Jobin Yvon Fluoromax-4 Spectrofluorometer. Commission Internationale de l'Eclairage (CIE) chromaticity coordinates and photoluminescence quantum efficiency were measured by the integrating sphere (F-3018) attached to the spectrofluorometer. The UV–vis diffuse reflectance spectra (DRS) were measured using a Hitachi U-3010 Spectrophotometer.

3. Results and discussions

3.1. X-ray diffraction

The powder X-ray diffraction (XRD) patterns of $Sr(La_{1-x}Eu_x)_2Mg_2W_2O_{12}$ ($x=0$, 0.10, 0.25, and 0.30) are shown in Fig. 1. For pure $SrLa_2Mg_2W_2O_{12}$, there is only one reported phase [19]. As shown in Fig. 1, when Eu^{3+} content is lower than 0.25, all XRD patterns can be indexed to orthorhombic perovskite $SrLa_2Mg_2W_2O_{12}$ (JCPDS#35-0259) and no impurities appear, indicating that Eu^{3+} has been successfully doped into the host crystal lattice. Diffraction peaks shift slightly to the higher angle with the increase of Eu^{3+} content (e.g. the enlarged XRD patterns ranging from 56° to 59° are shown in the right part of Fig. 1), which can be attributed to the replacement of the larger La^{3+} by relatively smaller Eu^{3+}, inducing a compacter lattice configuration. However, peaks belonging to $SrWO_4$ are observed with Eu^{3+} content ≥ 0.30, implying the occurrence of solubility saturation.

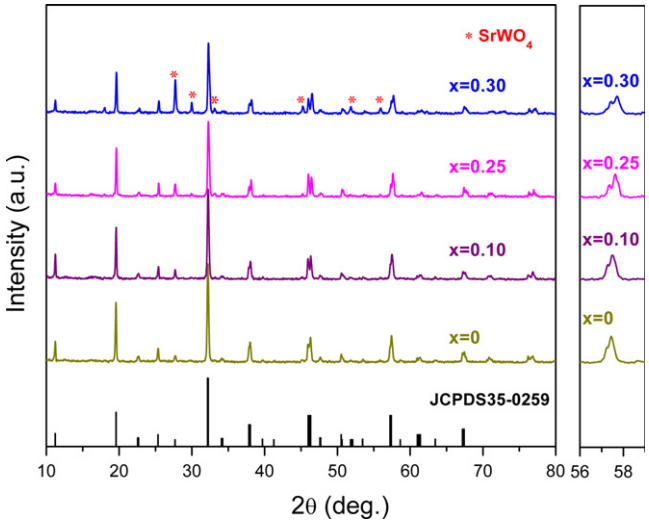

Fig. 1. XRD patterns of $Sr(La_{1-x}Eu_x)_2Mg_2W_2O_{12}$ ($x=0$, 0.10, 0.25, and 0.30) in the left side, and enlarged XRD patterns from 56° to 59° in the right side. Peaks caused by $SrWO_4$ are marked with '*' and the crystal indices are marked out together.

3.2. UV–vis DRS

The absorption spectra as well as the photoluminescence excitation (PLE) spectra of $Sr(La_{0.75}Eu_{0.25})_2Mg_2W_2O_{12}$ are shown in Fig. 2. In the PLE spectra, the peaks center at 395 nm, 464 nm and 533 nm are dominant, which can be attributed to Eu^{3+} ions 4f transitions $^7F_0$–$^5L_6$, $^7F_0$–$^5D_2$ and $^7F_0$–$^5D_1$ respectively. And those peaks have corresponding peaks in the absorption spectra demonstrated the close combination and cross-validation of the two parameters. In the absorption spectra, the peak at 395 nm is submerged into the absorption edge. All spectra shown in Fig. 2b have a large absorption edge between 300 nm and 400 nm, originating from the energy gap between the valance band and the empty conduction band. For pure $SrLa_2Mg_2W_2O_{12}$, the absorption edge is about 340 nm, indicating that the band gap is about 3.6 eV. With increased Eu^{3+} dopants, the absorption edge exhibits red shifts because of the overlap of Eu^{3+}–O^{2-} charge transfer band absorption and band gap absorption. Meanwhile, the absorption peaks at 464 nm and 533 nm, caused by the 4f transitions of Eu^{3+} ions, become more obvious, as the electron jump in Eu^{3+} increases the absorption of photon.

3.3. Luminescence properties

Luminescence properties of series of $Sr(La_{1-x}Eu_x)_2Mg_2W_2O_{12}$ are characterized in Fig. 3. The broad band

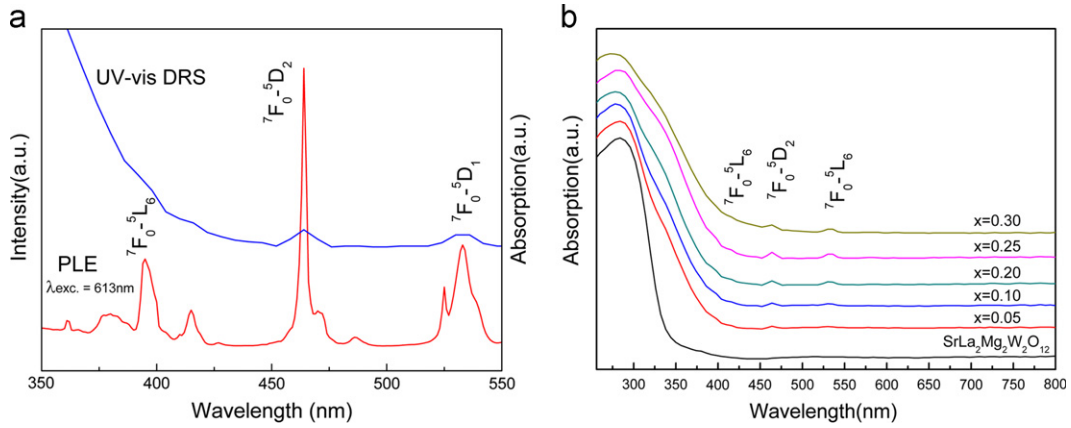

Fig. 2. (a) Absorption spectra and photoluminescence excitation spectra (with the monitoring wavelength of 613 nm) of $Sr(La_{0.75}Eu_{0.25})_2Mg_2W_2O_{12}$; and (b) absorption spectra of $Sr(La_{1-x}Eu_x)_2Mg_2W_2O_{12}$ (x=0, 0.05, 0.10, 0.20, 0.25, and 0.30).

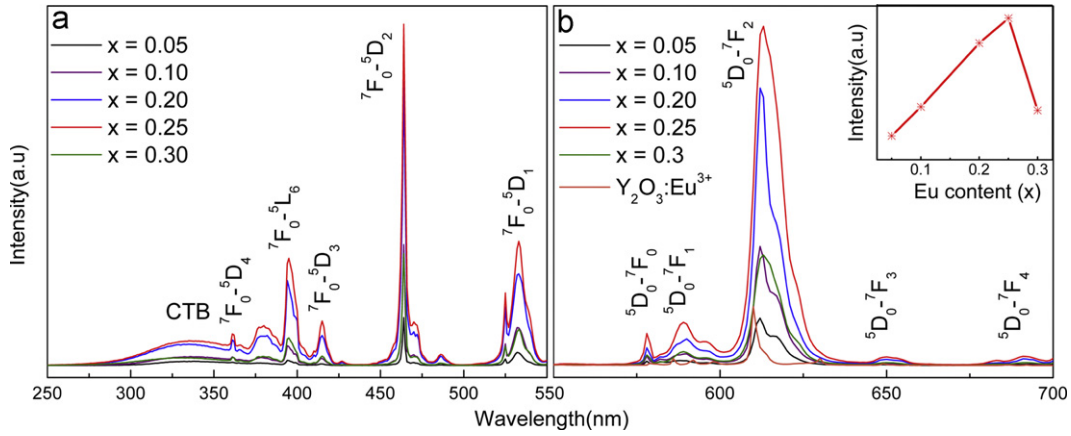

Fig. 3. (a) Photoluminescence excitation spectra (λ_{em}=613 nm) of $Sr(La_{1-x}Eu_x)_2Mg_2W_2O_{12}$ (x=0.05, 0.10, 0.20, 0.25, and 0.30); and (b) photoluminescence emission spectra of $Sr(La_{1-x}Eu_x)_2Mg_2W_2O_{12}$ (x=0.05, 0.10, 0.20, 0.25, and 0.30) (λ_{ex}=464 nm) and Y_2O_3:Eu^{3+} (λ_{ex}=466 nm), and the plot of the intensity from $^5D_0$–$^7F_2$ versus Eu^{3+} doping concentration for $Sr(La_{1-x}Eu_x)_2Mg_2W_2O_{12}$ in the inset diagram.

below 350 nm is attributed to the charge transfer (CT) transition between metal cations and oxygen anions [20,21]. The spectrum above 350 nm shows several sharp peaks, and all of them are attributed to the Eu^{3+} ions' characteristic 4f–4f transitions $^7F_0$–$^5D_4$, $^7F_0$–$^5L_6$, $^7F_0$–$^5D_3$, $^7F_0$–$^5D_2$ and $^7F_0$–$^5D_1$, respectively. The intensity of the highest peak observed at 464 nm is about 13.77 times stronger than that of the peak caused by CTB (charge transfer band), indicating that there is a weak non-radioactive absorption and high energy conversion. Peaks at 578 nm, 589 nm, 613 nm, 650 nm and 691 nm in emission spectra can be ascribed to $^5D_0$–^7F_J (J=0–4) transitions of Eu^{3+} ions from short to long wavelengths. The emission intensity induced by the $^5D_0$–$^7F_2$ of Eu^{3+} ions versus different Eu^{3+} doping concentrations are shown as the inset diagram in Fig. 3b. The highest intensity comes at x=0.25 and the intensity at 613 nm excited by 464 nm blue light is about three times higher than that of the commercial red phosphor Y_2O_3:Eu^{3+} at 615 nm (under 466 nm excitation).

As shown in Fig. 3b, under 464 nm blue light excitation, the emission intensity at 613 nm increases with Eu^{3+} doping concentration until the quenching effect appears at x=0.25. The intensity decreases sharply when Eu^{3+} ions concentration exceeds 0.25. Generally, the increase of active center (Eu^{3+} ions) helps the energy transfer as well as shortens the distance changes cross relaxation between neighboring Eu^{3+} defects, which lead to non-radioactive recombination and decrease the efficiency [22]. Hence there exists a balance point where emission intensity has a summit, which we call as the concentration quenching effect. The critical distance (R_c) is used to characterize the distance of Eu^{3+} ions when quenching effect appears. It can be calculated from samples' crystal structure parameters by the equation $R_c \approx 2(3V/4\pi xN)^{1/3}$ [23–25], where the volume of unit cell (V), critical concentration (x) and the number of total La^{3+} per unit cell (N) are needed. For $SrLa_2Mg_2W_2O_{12}$, V=486.3 Å^3, N=8, and x=0.25, so the calculated critical distance is about 7.74 Å, which is larger than 5 Å, indicating that the migration is hampered and the exchange interaction becomes ineffective [26]. Therefore, the high concentration quenching effect is possible in the $SrLa_2Mg_2W_2O_{12}$:xEu^{3+} system.

3.4. Quantum efficiencies and CIE chromaticity coordinates

To accurately investigate the luminescence properties of phosphors, the quantum efficiencies of $Sr(La_{0.75}Eu_{0.25})_2Mg_2W_2O_{12}$ was calculated using the method described by de Mello et al. [27] and Pålsson et al. [28], with commercial $Y_2O_3:Eu^{3+}$ as reference sample. In general, this method calculates the quantum efficiency (Φ_f) by measuring the integrated luminescence of the sample caused by direct excitation (E_c), the integrated luminescence from an empty integrating sphere (E_a), the integrated excitation profile from an empty integrating sphere (L_a), and the integrated excitation profile when the sample is directly excited by the incident beam (L_c). It also uses the equation $\Phi_f = N_{em}/N_{abs} = (E_c - E_a)/(L_a - L_c)$, where N_{em} and N_{abs} represent the emitted and absorbed photons of the samples respectively [29]. The quantum efficiencies of $Sr(La_{0.75}Eu_{0.25})_2Mg_2W_2O_{12}$ and $Y_2O_3:Eu^{3+}$ are listed in Table 1. When excited by 464 nm blue light, the $Sr(La_{0.75}Eu_{0.25})_2Mg_2W_2O_{12}$ shows a quantum efficiency of 27.1%, which is twice higher than the commercial phosphor (12.2%, excited by 466 nm blue light), indicating a good energy absorption and conversion property. The quantum efficiency of $Sr(La_{0.75}Eu_{0.25})_2Mg_2W_2O_{12}$ is higher when excited by blue light (464 nm), while slightly lower when excited by near-UV light (394 nm), which is consistent with the result shown in Table 1. Hence, it indicates that $Sr(La_{0.75}Eu_{0.25})_2Mg_2W_2O_{12}$ is more suitable for blue chips applications.

Fig. 4 shows the CIE chromaticity coordinate of $Sr(La_{0.75}Eu_{0.25})_2Mg_2W_2O_{12}$, yielding $x=0.660$, $y=0.340$, which is close to the standard of NTSC ($x=0.670$, $y=0.330$). The inset diagram at the top-right corner shows the $Sr(La_{0.75}Eu_{0.25})_2Mg_2W_2O_{12}$ powder photographed in the 365 nm Ultra-violet on a quartz slide in the dark room.

4. Conclusions

In this study, $Sr(La_{1-x}Eu_x)_2Mg_2W_2O_{12}$ phosphors were successfully synthesized using the high temperature solid state reaction method, and their luminescence properties were studied and discussed in detail. Eu^{3+}-doped $SrLa_2Mg_2W_2O_{12}$ phosphors show excellent red luminescent emission properties when excited by both blue and near-UV light. The $Sr(La_{0.75}Eu_{0.25})_2Mg_2W_2O_{12}$ has the strongest emission peak at 613 nm (excited by 464 nm light), which is about three times that of the commercial red phosphor $Y_2O_3:Eu^{3+}$ at 615 nm (excited by 466 nm light). Meanwhile, in this condition, its quantum efficiency is 27.1%, 2.22 times higher than $Y_2O_3:Eu^{3+}$. The calculated CIE chromaticity coordinate (0.660, 0.340) shows high color purity. All the results show that $Sr(La_{1-x}Eu_x)_2Mg_2W_2O_{12}$ is a promising high performance red emitting phosphor for WLEDs application.

Table 1
Quantum efficiencies of $Sr(La_{0.75}Eu_{0.25})_2Mg_2W_2O_{12}$ and $Y_2O_3:Eu^{3+}$ at different exciting wavelengths.

Samples	Exciting wavelength (nm)	Quantum efficiency (%)
$Sr(La_{0.75}Eu_{0.25})_2Mg_2W_2O_{12}$	464	27.1
	395	8.8
$Y_2O_3:Eu^{3+}$	466	12.2
	394	9.6

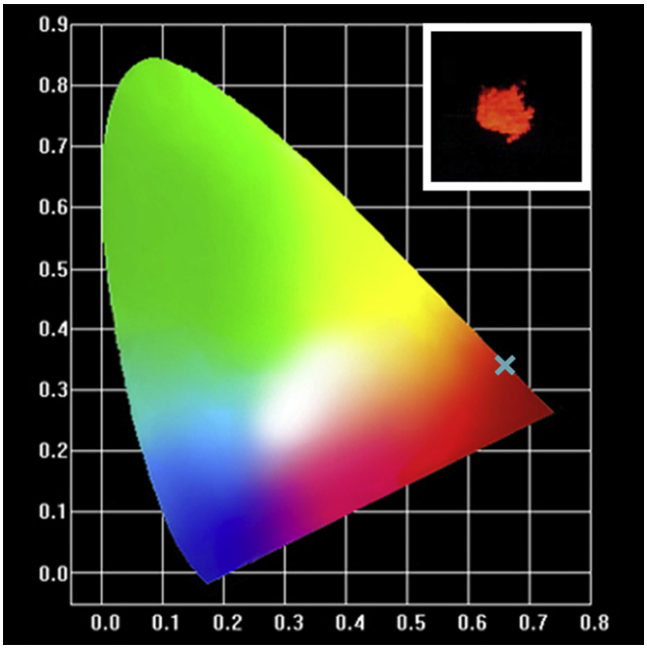

Fig. 4. The 1931 CIE chromaticity diagram of emission spectra excited by 464 nm blue light of $Sr(La_{0.75}Eu_{0.25})_2Mg_2W_2O_{12}$; and the inset diagram shows the image of $Sr(La_{0.75}Eu_{0.25})_2Mg_2W_2O_{12}$ under 365 nm UV.

Acknowledgment

This work is financially supported by NSF of China (Grant Nos. 51125006, 91122034, 51121064) and Innovation Program of the CAS(KJCX2-EW-W11).

References

[1] J. Hou, X. Yin, F. Huang, W. Jiang, Synthesis and photoluminescence properties of $NaLaMgWO_6:RE^{3+}$ (RE=Eu, Sm, Tb) phosphor for white LED application, Materials Research Bulletin 47 (6) (2012) 1295–1300.
[2] Z. Song, Y. Xu, C. Li, Y. Li, Z. Zhao, Z. Yang, D. Zhou, Z. Yin, H. Li, J. Qiu, Synthesis and photoluminescence properties of $MgAl(PO_4)O:Eu^{3+}$ red phosphor for white LEDs, Ceramics International (2012).
[3] E.F. Schubert, J.K. Kim, H. Luo, J.Q. Xi, Solid-state lighting—a benevolent technology, Reports on Progress in Physics 69 (12) (2006) 3069–3099.
[4] J.T. Wessels, U. Pliquett, F.S. Wouters, Light-emitting diodes in modern microscopy—from David to Goliath?, Cytometry Part A: The Journal of the International Society for Analytical Cytology 81 (3) (2012) 188–197.

[5] T. Justel, H. Nikol, C. Ronda, New developments in the field of luminescent materials for lighting and displays, Angewandte Chemie-Internaional Edition 37 (22) (1998) 3085–3103.
[6] M. Bredol, U. Kynast, C. Ronda, Designing luminescent materials, Advanced Materials 3 (7–8) (1991) 361–367.
[7] M.H. Crawford, LEDs for solid-state lighting: performance challenges and recent advances, IEEE Journal of Selected Topics in Quantum Electronics 15 (4) (2009) 1028–1040.
[8] X. Zhang, X. Wang, J. Huang, J. Shi, M. Gong, Near UV-based LED fabricated with $Ba_5SiO_4(F,Cl)_6:Eu^{2+}$ as blue- and green-emitting phosphor, Optical Materials 32 (1) (2009) 75–78.
[9] J.K. Park, M.A. Lim, C.H. Kim, H.D. Park, J.T. Park, S.Y. Choi, White light-emitting diodes of GaN-based Sr_2SiO_4:Eu and the luminescent properties, Applied Physics Letters 82 (5) (2003) 683–685.
[10] X.Q. Piao, T. Horikawa, H. Hanzawa, K. Machida, Characterization and luminescence properties of $Sr_2Si_5N_8:Eu^{2+}$ phosphor for white light-emitting-diode illumination, Applied Physics Letters 88 (16) (2006) 161908 161903.
[11] J.S. Kim, P.E. Jeon, Y.H. Park, J.C. Choi, H.L. Park, G.C. Kim, T.W. Kim, White-light generation through ultraviolet-emitting diode and white-emitting phosphor, Applied Physics Letters 85 (17) (2004) 3696–3698.
[12] S. Shionoya, W.M. Yen, H. Yamamoto, in: Phosphor Handbook, 2nd ed., CRC Press, New York, 2006.
[13] R.J. Xie, N. Hirosaki, Y.Q. Li, T. Takeda, Rare-earth activated nitride phosphors: synthesis, luminescence and applications, Materials 3 (6) (2010) 3777–3793.
[14] C.F. Guo, B.L. Chu, Q. Su, Improving the stability of alkaline earth sulfide-based phosphors, Applied Surface Science 225 (1–4) (2004) 198–203.
[15] S.L. Jones, D. Kumar, R.K. Singh, P.H. Holloway, Luminescence of pulsed laser deposited Eu doped yttrium oxide films, Applied Physics Letters 71 (3) (1997) 404–406.
[16] X. Yin, Y. Wang, D. Wan, F. Huang, J. Yao, Red-luminescence enhancement of ZrO_2-based phosphor by codoping Eu^{3+} and M^{5+} (M = Nb, Ta), Optical Materials 34 (8) (2012) 1353–1356.
[17] Y. Su, L. Li, G. Li, Synthesis and optimum luminescence of $CaWO_4$-based red phosphors with codoping of Eu^{3+} and Na, Chemistry of Materials 20 (19) (2008) 6060–6067.
[18] Y. Zhang, N.A.W. Holzwarth, R.T. Williams, Electronic band structures of the scheelite materials $CaMoO_4$, $CaWO_4$, $PbMoO_4$, and $PbWO_4$, Physical Review B 57 (20) (1998) 12738–12750.
[19] Y. Torii, Synthesis and defect structure of $SrLa_2(Mg_2W_2)O_{12}$ and $Sr_2La_2(MgW_2)O_{12}$, Chemistry Letters 8 (11) (1979) 1393–1396.
[20] X. Yin, Y. Wang, F. Huang, Y. Xia, D. Wan, J. Yao, Excellent red phosphors of double perovskite Ca_2LaMO_6:Eu (M = Sb, Nb, Ta) with distorted coordination environment, Journal of Solid State Chemistry 184 (12) (2011) 3324–3328.
[21] D. Huang, Y. Zhou, W. Xu, Z. Yang, M. Hong, J. Yu, Synthesis and luminescent properties of $Na_5La_{1-x}Eu_x(WO_4)_4$ red phosphors, Journal of Luminescence 132 (10) (2012) 2788–2793.
[22] P.K. Sharma, R. Nass, H. Schmidt, Effect of solvent, host precursor, dopant concentration and crystallite size on the fluorescence properties of Eu(III) doped yttria, Optical Materials 10 (2) (1998) 161–169.
[23] G. Blasse, Energy transfer in oxidic phosphors, Physics Letters A 28 (6) (1968) 444–445.
[24] X. Yin, J. Yao, Y. Wang, C. Zhao, F. Huang, Novel red phosphor of double perovskite compound La_2MgTiO_6:xEu^3, Journal of Luminescence 132 (7) (2012) 1701–1704.
[25] W.B. Im, N.N. Fellows, S.P. DenBaars, R. Seshadri, Y.-I. Kim, LaSr2AlO5, a versatile host compound for Ce^{3+}-based yellow phosphors: structural tuning of optical properties and use in solid-state white lighting, Chemistry of Materials 21 (13) (2009) 2957–2966.
[26] G. Blasse, B.C. Grabmaier, Luminescent Materials, Springer-Verlag, Berlin and New York, 1994.
[27] J.C. de Mello, H.F. Wittmann, R.H. Friend, An improved experimental determination of external photoluminescence quantum efficiency, Advanced Materials 9 (3) (1997) 230–232.
[28] L.O. Pålsson, A.P. Monkman, Measurements of solid-state photoluminescence quantum yields of films using a fluorimeter, Advanced Materials 14 (10) (2002) 757.
[29] J. Hou, X. Yin, Y. Fang, F. Huang, W. Jiang, Novel red-emitting perovskite-type phosphor $CaLa_{1-x}MgM'O_6$:xEu^{3+} (M′ = Nb, Ta) for white LED application, Optical Materials 34 (8) (2012) 1394–1397.